UDC 621.3 https://doi.org/10.20998/2074-272X.2022.6.07

A.A. Bengharbi, S. Laribi, T. Allaoui, A. Mimouni

Photovoltaic system faults diagnosis using discrete wavelet transform based artificial neural networks

Introduction. *This research work focuses on the design and experimental validation of fault detection techniques in grid-connected solar photovoltaic system operating under Maximum Power Point Tracking mode and subjected to various operating conditions.* ***Purpose.*** *Six fault scenarios are considered in this study including partial shading, open circuit in the photovoltaic array, complete failure of one of the six IGBTs of the inverter and some parametric faults that may appear in controller of the boost converter.* ***Methods.*** *The fault detection technique developed in this work is based on artificial neural networks and uses discrete wavelet transform to extract the features for the identification of the underlying faults. By applying discrete wavelet transform, the time domain inverter output current is decomposed into different frequency bands, and then the root mean square values at each frequency band are used to train the neural network.* ***Results.*** *The proposed fault diagnosis method has been extensively tested on the above faults scenarios and proved to be very effective and extremely accurate under large variations in the irradiance and temperature.* ***Practical significance.*** *The results obtained in the binary numerical system allow it to be used as a machine code and the simulation results has been validated by MATLAB / Simulink software.* References 21, tables 5, figures 7.

Key words: **artificial neural network, discrete wavelet transform, fault diagnosis, photovoltaic system.**

Вступ. *Ця дослідницька робота присвячена розробці та експериментальній перевірці методів виявлення несправностей у підключеній до мережі сонячній фотоелектричній системі, що працює в режимі відстеження точки максимальної потужності та піддається різним умовам експлуатації.* ***Мета***. *У цьому дослідженні розглядаються шість сценаріїв відмови, включаючи часткове затінення, обрив кола у фотогальванічній батареї, повна відмова одного з шести IGBT інвертора та деякі параметричні відмови, які можуть виникнути в контролері перетворювача, що підвищує.* ***Методи***. *Методика виявлення несправностей, розроблена у цій роботі, полягає в штучних нейронних мережах і використовує дискретне вейвлет-перетворення для отримання ознак для ідентифікації основних несправностей. Застосовуючи дискретне вейвлет-перетворення, вихідний струм інвертора в часовій області розкладається на різні смуги частот, а потім середньоквадратичні значення в кожній смузі частот використовуються для навчання нейронної мережі.* ***Результати***. *Запропонований метод діагностики несправностей був всебічно протестований на вказаних вище сценаріях несправностей і виявився дуже ефективним і надзвичайно точним при великих коливаннях освітленості і температури.* ***Практична значимість***. *Результати, отримані в двійковій системі числення, дозволяють використовувати її як машинний код, а результати моделювання були підтверджені програмним забезпеченням MATLAB/Simulink.* Бібл. 21, табл. 5, рис. 7.

Ключові слова: **штучна нейронна мережа, дискретне вейвлет-перетворення, діагностика несправностей, фотоелектрична система.**

Abbreviations

ANN	Artificial neural network	MPPT	Maximum power point tracking
CNN	Convolutional neural networks	PLL	Phase lock loop
CWT	Continuous wavelet transform	PSO	Particle swarm optimization
DWT	Discrete wavelet transform	PV	Photovoltaic
HF	High frequency	RMS	Root mean square
HPF	High-pass filter	SVPWM	Space vector pulse width modulation
LF	Low frequency	VOC	Vector oriented control
LPF	Low-pass filter	WT	Wavelet transform

Introduction. Global energy demand is rising at a fast pace and CO_2 emissions have reached their highest record in recent years; which has prompted the industrialized world to search for alternative energies resources to overcome the declining fossil fuel reserves. Solar PV energy is one of the most promising renewable energies sources [1]. Therefore, PV power generation has become so mainstream and usually is distributed in some distant and cruel environments, and because some faults are inevitable during the long-term operation of the PV system it has become clear that PV system require to be better protected against faults [2, 3]. Also the electrical faults and interconnected power system increases the cost and emission ratio very high [4].

Detecting faults of the PV components and fix it is necessary to avoid economic losses and big incidents that may established in this systems, thus ensuring secure and robust systems [5]. Moreover, more time and costs are suffered when malfunction is failed to be detected in a timely manner in the system. Therefore, to ensure a high-quality system for prolonged, it is essential to recognize the times and locations of faults and failures immediately [5].

Since diagnosing faults is essential to the PV systems, over the past few years researchers have become increasingly interested in diagnosing complex system faults. A large number of fault diagnostic methods and several approaches have been proposed by researchers. In [6] a new PV array fault diagnosis technique capable of automatically extracting features from raw data for PV array fault classification was proposed. That technique shows good fault diagnosis precision on both noisy and noiseless data. In [7], a technique for the rapid detection and isolation of faults in the DC micro-grids without deactivating the entire network has been introduced. The technique is based on sampling branch current measurements then using WT to capture the features from the network current signals. The authors in [8] presented a new approach to effectively classify and detect PV system faults using deep two-dimensional (2-D) CNN to extract features from 2-D scalograms generated from PV system data. In [9], the authors propose a recurrent neural network-based long short-term memory approach for the detection of high impedance fault in PV integrated power system. In [10], a CNN was combined with a chaotic system

© A.A. Bengharbi, S. Laribi, T. Allaoui, A. Mimouni

and the DWT and applied to the diagnosis of insulation faults in cross-linked polyacetylene power cables. The method presented in [11] is based on the combination of an ANN with WT and leads to an accurate fault location strategy in bipolar current source converter based high voltage DC transmission system. In [12], a design of a monitoring system using a perceptron multilayer ANN for the detection of rolling element-bearings failure was proposed. The authors in [13] applied WT to extract the features of fault signals then used them for training an ANN that can classify and detect faults in DC microgrid.

Many techniques are used to detecting the faults in the PV systems, from the above we note that fault detection is directly dependent on signal current or voltage which is sensed using sensors and sampled for further process. Next, effective and different feature extraction techniques are used in the discussed fault detection methods to obtain the most versatile and effective features possible.

The objective of this work is to create an artificial neural network observer that can detect and classify faults in photovoltaic system. By using DWT on real data of PV system under different operating conditions with and without faults in order to extract the features then learn and train the ANN with these features.

Materials and methods. The experimental grid-connected PV system used in this study is depicted in Fig. 1 and its presentation with the proposed fault detection method – in Fig. 2.

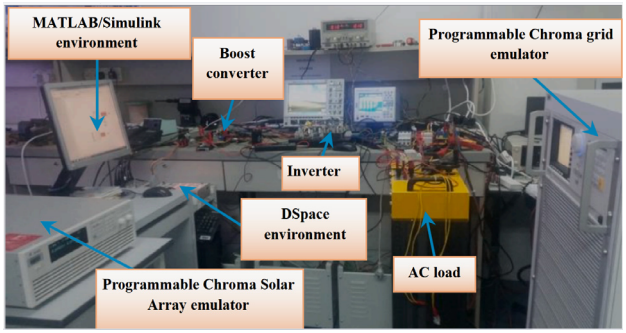

Fig. 1. Depict implemented grid-connected PV system [14]

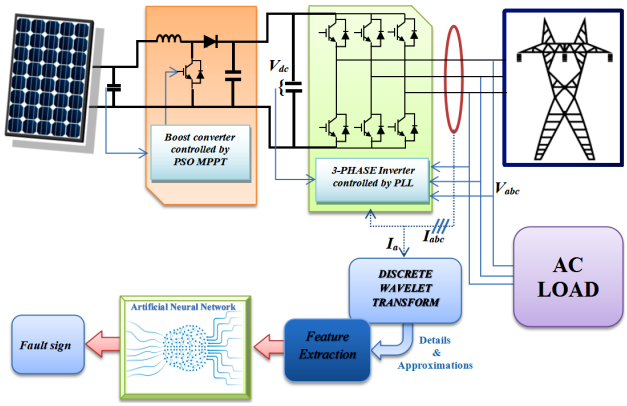

Fig. 2. Presentation of implemented grid-connected PV system with the proposed fault detection method

A typical grid-connected PV system implemented in the laboratory is used to verify the fault detection performance of data dependent methods against real faults in practical conditions and MPPT mode. The output of the PV array is created by the programmable Chroma 62150H-1000S Solar Array emulator which allows modifies the effects of peripheral conditions (irradiance G and temperature T), and as a grid emulator The programmable AC source Chroma 61,511. A DSpace 1104 environment implement the control algorithm and used also for data acquisition. Based on the grid-side signals, VOC based on SVPWM is used to control the active and reactive powers. The inverter output voltage is synchronized with the grid voltage through the PLL. For safety and protection purposes, the AC load is used when real faults are applied. To extract maximum power from the PV array, a MPPT controller based on PSO technique is used [14].

Therefore, this system was used to create and collect real faulty data for fault detection experimental validation; we refer interested readers to [15, 16] for more details on settings of this system. the PV array voltage V_{PV} and current I_{PV} and DC voltage V_{dc} as shown in Fig. 1, are real-time measured signals with a sampling time of $T_s = 100$ µs [14].

The minimum set of variables associated with faults is: $\{I_{PV}, V_{PV}, V_{dc}, |I|, f_I, |V|, f_V\}$, where f_I, f_V are current and voltage frequency. It used for observing the PV system.

The real-time measured and estimated signals form a data matrix Y of 7 columns:

$$Y = [I_{PV} \;\; V_{PV} \;\; V_{dc} \;\; |I| \;\; f_I \;\; |V| \;\; f_V]^T. \qquad (1)$$

This work considers the detection of the 6 factual faults listed in Table 1 that were injected into the PV system. The faults are of different types and locations and are injected manually in separate experiments to ensure an entire analysis. Each trial lasts about 10 to 15 s where in the fault is applied around the 7th to 9th s. Degradation faults are not considered in this work, as their detection requires long-term data at large sampling time intervals [14].

Table 1

Realistic injected fault in the PV system [14]

Fault	Type	Description
F1	Inverter fault	Complete failure in one of the six IGBTs
F2	Feedback sensor fault	One phase sensor fault 20%
F3	PV array mismatch	10 to 20% non homogeneous partial shading
F4	PV array mismatch	15% open circuit in PV array
F5	MPPT controller fault	–20% gain parameter of PI controller in MPPT controller of the boost converter
F6	Boost converter controller fault	+20% in time constant parameter of PI controller in MPPT controller of the boost converter

Proposed fault detection strategy. The proposed fault detection method is described by the flowchart of Fig. 3. The fault diagnosis algorithm uses the inverter output current signals for feature extraction approach based on the DWT. The aim of signal processing is to extract the features of the signal from several angles through several transform methods to aid in signal analysis and processing. The wavelet function is a new foundation for expressing signals and a good method for analyzing the signal from different resolutions [10].

Feature extraction using wavelet transform. Feature extraction is the most important part in the proposed fault detection and classification process.

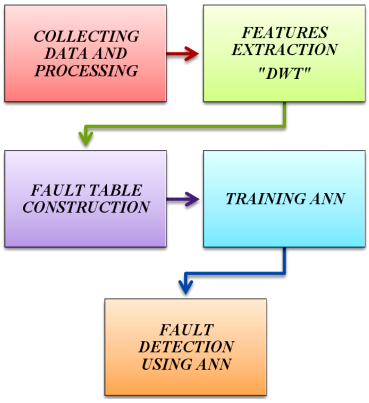

Fig. 3. Flowchart of the proposed fault detection system

Better features lead to improved system performance and reliability, because the accuracy of a system depends on the quality and robustness of the feature extraction process. Wavelet transform is a mathematical tool for temporal frequency analysis and has been used in several fault detection applications. It is based on the transformation of the temporal signal into a series of parameters called approximation and detail representing the slow and fast changes in the signal, respectively. The wavelets are defined as follows [17]:

$$\Psi_{ab}(t)=\frac{1}{\sqrt{a}}\cdot\Psi\left(\frac{t-b}{a}\right), \tag{2}$$

where a and b are the scale factor and position factor respectively.

Wavelet transform is divided into CWT and DWT [10]. The DWT algorithm translates and dilates the wavelet according to discrete values. Therefore, a and b will be discretized as follows [18]:

$$\begin{cases} a=a_0^m; \\ b=n\cdot b_0\cdot a_0^m, \end{cases} \tag{3}$$

where $a_0 > 1$, $b_0 > 0$; a_0 and $b_0 \in Z$; m and n are the integers permitting the control of the dilation and the translation of the original wavelet [17].

The DWT algorithm is used to eliminate noise in the original signal and also to decompose the time domain signal into different frequency groups. The original signal $f(t)$ passes through two complementary filters: a HPF and a LPF appear as two signals defined as the approximation signal ***A*** and the detail signal ***D*** as shown in Fig. 4.

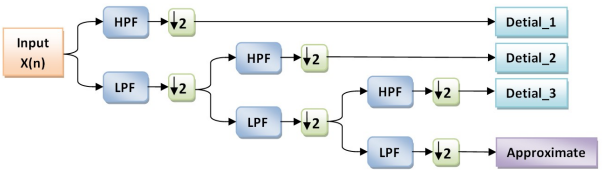

Fig. 4. DWT implementation procedure

The approximation is the large-scale and the low frequency part of the signal and the detail is the small-scale and high frequency part of the signal [18].

Through DWT, the input signals which consist of LF and HF components can be decomposed into frequency bands. Then, through down-sampling, the first level of wavelet transform can be obtained [10].

For a reliable and fast analysis, a prior knowledge of the signal levels N to be processed is necessary. The following equation gives this required parameter [17]:

$$N_{levels}=\text{int}\left(\frac{\log\left(f_e/f_s\right)}{\log 2}\right)+2\,, \tag{4}$$

where f_s is the supply frequency; f_e is the sampling frequency. Note that N_{levels} should be an integer.

The appropriate decompositions number can calculated based on the knowledge of f_s and f_e. In our case, considering a supply frequency of 50 Hz and a sampling frequency of 10 kHz, the number of decomposition levels required is [17]:

$$N_{levels}=n_{ls}+2=\text{int}\left(\frac{\log\left(10^4/50\right)}{\log 2}\right)+2=9 \text{ levels.} \tag{5}$$

Table 2 presents the different frequency bands acquired by the discrete wavelet decomposition. Figure 5 shows the DWT that implemented to decompose the current signal (i_a) in MATLAB/Simulink environment to obtained the Details.

Table 2

Frequency bands obtained by multi-level decomposition

Levels	Approximations		Details	
J=1	A1	0-5000	D1	5000-10000
J=2	A2	0-2500	D2	2500-5000
J=3	A3	0-1250	D3	1250-2500
J=4	A4	0-625	D4	625-1250
J=5	A5	0-312.5	D5	312.5-625
J=6	A6	0-156.25	D6	156.25-312.5
J=7	A7	0-78.125	D7	78.125-156.25
J=8	A8	0-39.0625	D8	39.0625-78.125
J=9	A9	0-19.5313	D9	19.5313-39.0625

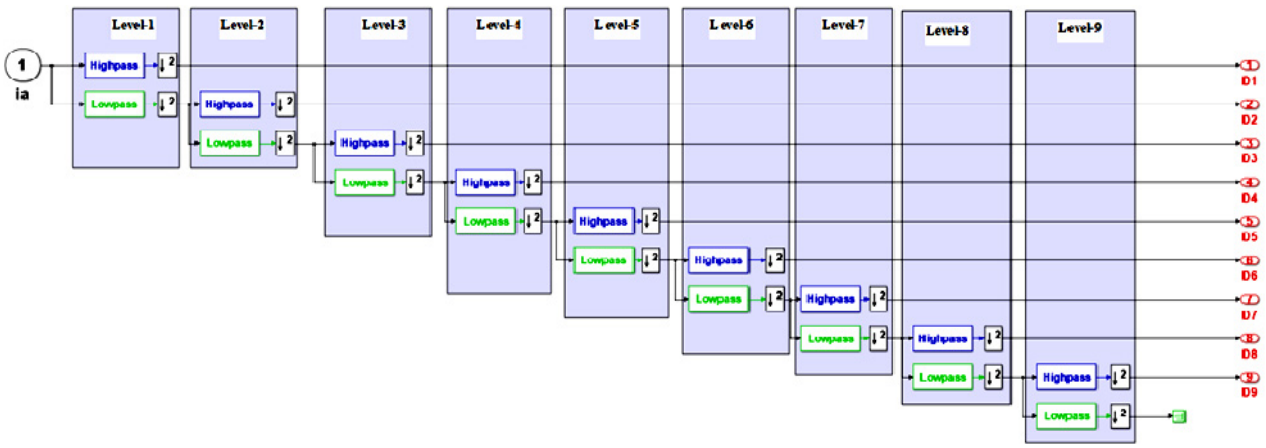

Fig. 5. DWT implemented in MATLAB / Simulink environment

Figure 6,*a* shows the inverter output current (i_a) in healthy case, and in Fig. 6,*c* in faulty case (F1).

Different details extracted from the obtained inverter output current signal by the DWT technique for the healthy case in Fig. 6,*b* and the faulty case in Fig. 6,*d* (F1) is displayed below. By comparing healthy case details and faulty case (F1) Details of the PV system state as depicted in Fig. 6,*b* and Fig. 6,*d* a remarkable variation in details amplitude is observed.

Note that these statements are valid for the other faulty cases when we compare it with the healthy case.

The variation in those details provides some useful information in the signal to extract and use it to train ANN.

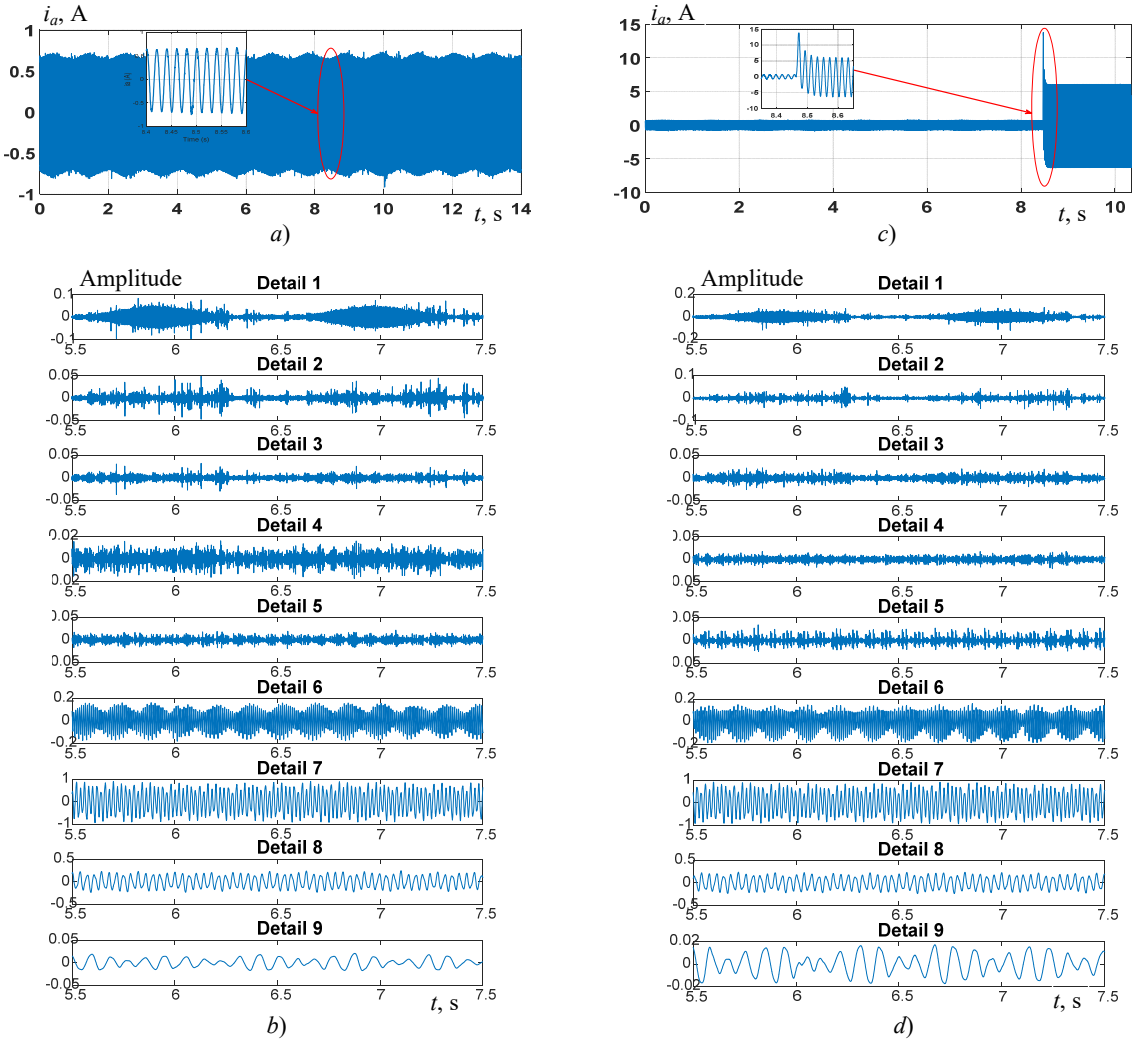

Fig. 6. Inverter output current (i_a) and its details in healthy and faulty cases

Fault table based on extracted features. The next process is to create a fault table according to feature values under each fault by using the RMS of each detail:

$$RMS = \sqrt{\frac{1}{n}\sum_i x_i^2}\ , \qquad (6)$$

where x_i denotes the measurements and n is the number of measurements.

We should carefully observed these feature values because these values will use for training. Using this fault Table 3, an ANN is trained and then used to identify the faults.

Table 3

Fault table based on extracted features

	$D1_{RMS}$	$D2_{RMS}$	$D3_{RMS}$	$D4_{RMS}$	$D5_{RMS}$	$D6_{RMS}$	$D7_{RMS}$	$D8_{RMS}$	$D9_{RMS}$
Healthy	0.0167	0.0040	0.0038	0.0042	0.0058	0.0798	0.4734	0.1243	0.0142
F1	0.0132	0.0034	0.0037	0.0092	0.0229	0.2653	1.5706	0.4442	0.1148
F2	0.0172	0.0042	0.0041	0.0044	0.0061	0.0808	0.4832	0.1268	0.0132
F3	0.0173	0.0053	0.0040	0.0042	0.0075	0.0624	0.3529	0.0925	0.0094
F4	0.0162	0.0042	0.0034	0.0037	0.0056	0.0637	0.3744	0.0981	0.0109
F5	0.0172	0.0045	0.0045	0.0049	0.0091	0.0869	0.4644	0.1219	0.0127
F6	0.0173	0.0045	0.0045	0.0048	0.0094	0.0900	0.4759	0.1250	0.0108

Artificial neural network. The Artificial neural network system has proven its capability in a variety of engineering applications such as estimation, process control and diagnostics [19].

ANN is modeled on the human brain and nervous system. It requires to train and calculate hidden layer weights according to the inputs and required outputs before using it in a specific system. It consists of the input layer, hidden layer or layers, and an output layer. Weights of hidden nodes are calculated during the training process to provide the exact output in case of same or nearly equal input combinations. Back-propagation technique is used for weight training of neural network; this method calculates the gradient of a loss function with respect to all weights in the network so that the gradient is fed to the optimization method which uses it to update weights in an attempt to minimize loss function [20].

The ANN architecture employed in this work is shown in Fig. 7. It consists of the input layer with 9 neurons, one for each RMS detail, a hidden layer with 10 neurons, and an output layer with 4 neurons referring to the sign of the fault we want to detect. The back-propagation technique used for training is based on Levenberg-Marquardt algorithm. The sigmoid activation function is used for hidden and output layers.

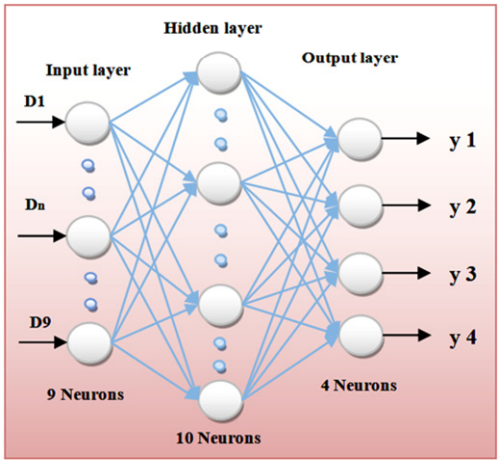

Fig. 7. ANN Structure

Table 4 represents the corresponding sign to each fault; the sign consist of 4 variables in binary numerical system which indicates to fault number ("***F***"*n*) in decimal numerical system. The objective of using the binary numerical system as target output is to use it as machine code.

Table 4

Fault sign

	y1	y2	y3	y4	Decimal N°
Healthy	0	0	0	0	0
F1	1	0	0	0	1
F2	0	1	0	0	2
F3	1	1	0	0	3
F4	0	0	1	0	4
F5	1	0	1	0	5
F6	0	1	1	0	6

Results and discussion. First of all, the ANN must be trained with healthy and faulty data. Then this trained neural network is used for fault detection system.

MATLAB/Simulink neural network toolbox is used to train the neural network according to the extracted features shown in Table 3 and the sign given in Table 4. The training process is simple and easy to perform using the MATLAB toolbox. The trained neural network can be easily converted to Simulink blocks or a MATLAB function which can be readily integrated in our designed system.

At the end of the training process, the model obtained consists of the optimal weight and the bias vector. The minimum performance gradient was set and training will stop when any one of conditions is met.

An automatic learning of the ANN is performed until a mean squared error of $2.1884 \cdot 10^{-22}$ is obtained at epoch 13.

Table 5 represents the obtained results in MATLAB/Simulink environment; it shows that the results are similar to the target output in Table 4.

Table 5

Tests results

Healthy	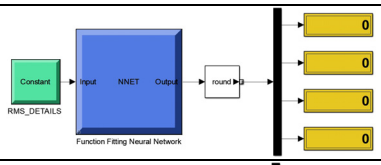	0
F1	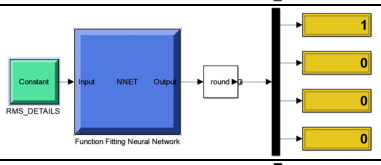	1
F2	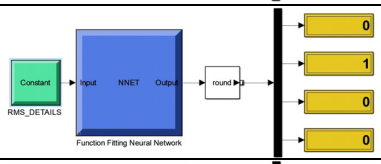	2
F3	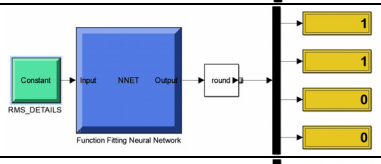	3
F4	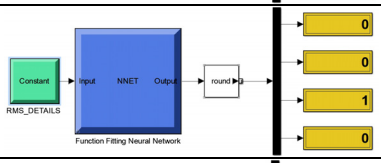	4
F5	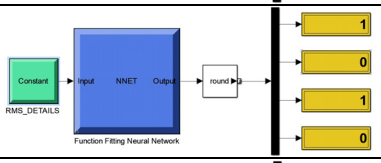	5
F6	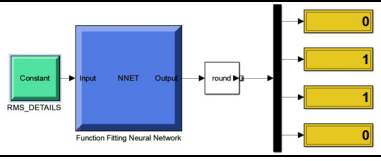	6

Conclusion. In this research work, we presenting a study of diagnostic technique for PV system based on real data, using wavelet transform and artificial neurons network. This study aims to find a solution to an effective and robust detection faults in the PV system such as partial shading, an open-circuit of the PV array of the system, a complete failure in one of the six IGBTs of the inverter and some parametric faults.

This technique shows a good performance. Furthermore, the simplicity of this proposed algorithm also shortens the response time, that's why it can detect the faults with high speed and accuracy.

Appendix. Reference [21] represents the grid-connected PV system faults data that are collected from lab experiments of faults in a PV microgrid system. There

are 16 data files in '.mat' form and also '.csv' form. Experimental data files are available in [21].

Acknowledgment. The authors would like to thank A. Bakdi, A. Guichi, S. Mekhilef and W. Bounoua for providing grid-connected PV system faults data from lab experiments which was part of this research work.

Conflict of interest. The authors declare no conflict of interest.

REFERENCES

1. Eltawil M.A., Zhao Z. MPPT techniques for photovoltaic applications. *Renewable and Sustainable Energy Reviews*, 2013, vol. 25, pp. 793-813. doi: https://doi.org/10.1016/j.rser.2013.05.022.

2. Albers M.J., Ball G. Comparative Evaluation of DC Fault-Mitigation Techniques in Large PV Systems. *IEEE Journal of Photovoltaics*, 2015, vol. 5, no. 4, pp. 1169-1174. doi: https://doi.org/10.1109/JPHOTOV.2015.2422142.

3. Liu S., Dong L., Liao X., Cao X., Wang X., Wang B. Application of the Variational Mode Decomposition-Based Time and Time–Frequency Domain Analysis on Series DC Arc Fault Detection of Photovoltaic Arrays. *IEEE Access*, 2019, vol. 7, pp. 126177-126190. doi: https://doi.org/10.1109/ACCESS.2019.2938979.

4. Akbar F., Mehmood T., Sadiq K., Ullah M.F. Optimization of accurate estimation of single diode solar photovoltaic parameters and extraction of maximum power point under different conditions. *Electrical Engineering & Electromechanics*, 2021, no. 6, pp. 46-53. doi: https://doi.org/10.20998/2074-272X.2021.6.07.

5. Kim G.G., Lee W., Bhang B.G., Choi J.H., Ahn H.-K. Fault Detection for Photovoltaic Systems Using Multivariate Analysis With Electrical and Environmental Variables. *IEEE Journal of Photovoltaics*, 2021, vol. 11, no. 1, pp. 202-212. doi: https://doi.org/10.1109/JPHOTOV.2020.3032974.

6. Appiah A.Y., Zhang X., Ayawli B.B.K., Kyeremeh F. Long Short-Term Memory Networks Based Automatic Feature Extraction for Photovoltaic Array Fault Diagnosis. *IEEE Access*, 2019, vol. 7, pp. 30089-30101. doi: https://doi.org/10.1109/ACCESS.2019.2902949.

7. Jayamaha D.K.J.S., Lidula N.W.A., Rajapakse A.D. Wavelet-Multi Resolution Analysis Based ANN Architecture for Fault Detection and Localization in DC Microgrids. *IEEE Access*, 2019, vol. 7, pp. 145371-145384. doi: https://doi.org/10.1109/ACCESS.2019.2945397.

8. Aziz F., Ul Haq A., Ahmad S., Mahmoud Y., Jalal M., Ali U. A Novel Convolutional Neural Network-Based Approach for Fault Classification in Photovoltaic Arrays. *IEEE Access*, 2020, vol. 8, pp. 41889-41904. doi: https://doi.org/10.1109/ACCESS.2020.2977116.

9. Veerasamy V., Wahab N.I.A., Othman M.L., Padmanaban S., Sekar K., Ramachandran R., Hizam H., Vinayagam A., Islam M.Z. LSTM Recurrent Neural Network Classifier for High Impedance Fault Detection in Solar PV Integrated Power System. *IEEE Access*, 2021, vol. 9, pp. 32672-32687. doi: https://doi.org/10.1109/ACCESS.2021.3060800.

10. Wang M.-H., Lu S.-D., Liao R.-M. Fault Diagnosis for Power Cables Based on Convolutional Neural Network With Chaotic System and Discrete Wavelet Transform. *IEEE Transactions on Power Delivery*, 2022, vol. 37, no. 1, pp. 582-590. doi: https://doi.org/10.1109/TPWRD.2021.3065342.

11. Ankar S., Sahu U., Yadav A. Wavelet-ANN Based Fault Location Scheme for Bipolar CSC-Based HVDC Transmission System. *2020 First International Conference on Power, Control and Computing Technologies (ICPC2T)*, 2020, pp. 85-90. doi: https://doi.org/10.1109/ICPC2T48082.2020.9071450.

12. Souad S.L., Azzedine B., Meradi S. Fault diagnosis of rolling element bearings using artificial neural network. *International Journal of Electrical and Computer Engineering (IJECE)*, 2020, vol. 10, no. 5, pp. 5288-5295. doi: https://doi.org/10.11591/ijece.v10i5.pp5288-5295.

13. Jayamaha D.K.J., Lidula N.W., Rajapakse A. Wavelet Based Artificial Neural Networks for Detection and Classification of DC Microgrid Faults. *2019 IEEE Power & Energy Society General Meeting (PESGM)*, 2019, pp. 1-5. doi: https://doi.org/10.1109/PESGM40551.2019.8974108.

14. Bakdi A., Bounoua W., Guichi A., Mekhilef S. Real-time fault detection in PV systems under MPPT using PMU and high-frequency multi-sensor data through online PCA-KDE-based multivariate KL divergence. *International Journal of Electrical Power & Energy Systems*, 2021, vol. 125, art. no. 106457. doi: https://doi.org/10.1016/j.ijepes.2020.106457.

15. Guichi A., Talha A., Berkouk E.M., Mekhilef S., Gassab S. A new method for intermediate power point tracking for PV generator under partially shaded conditions in hybrid system. *Solar Energy*, 2018, vol. 170, pp. 974-987. doi: https://doi.org/10.1016/j.solener.2018.06.027.

16. Bakdi A., Bounoua W., Mekhilef S., Halabi L.M. Nonparametric Kullback-divergence-PCA for intelligent mismatch detection and power quality monitoring in grid-connected rooftop PV. *Energy*, 2019, vol. 189, art. no. 116366. doi: https://doi.org/10.1016/j.energy.2019.116366.

17. Eddine C.B.D., Azzeddine B., Mokhtar B. Detection of a two-level inverter open-circuit fault using the discrete wavelet transforms technique. *2018 IEEE International Conference on Industrial Technology (ICIT)*, 2018, pp. 370-376. doi: https://doi.org/10.1109/ICIT.2018.8352206.

18. Souad L., Azzedine B., Eddine C.B.D., Boualem B., Samir M., Youcef M. Induction machine rotor and stator faults detection by applying the DTW and N-F network. *2018 IEEE International Conference on Industrial Technology (ICIT)*, 2018, pp. 431-436. doi: https://doi.org/10.1109/ICIT.2018.8352216.

19. Bouchaoui L., Hemsas K.E., Mellah H., Benlahneche S. Power transformer faults diagnosis using undestructive methods (Roger and IEC) and artificial neural network for dissolved gas analysis applied on the functional transformer in the Algerian north-eastern: a comparative study. *Electrical Engineering & Electromechanics*, 2021, no. 4, pp. 3-11. doi: https://doi.org/10.20998/2074-272X.2021.4.01.

20. Talha M., Asghar F., Kim S.H. A Novel Three-Phase Inverter Fault Diagnosis System Using Three-dimensional Feature Extraction and Neural Network. *Arabian Journal for Science and Engineering*, 2019, vol. 44, no. 3, pp. 1809-1822. doi: https://doi.org/10.1007/s13369-018-3156-8.

21. Bakdi A., Guichi A., Mekhilef S., Bounoua W. GPVS-Faults: Experimental Data for fault scenarios in grid-connected PV systems under MPPT and IPPT modes, *Mendeley Data*, 2020, V1. doi: https://dx.doi.org/http://dx.doi.org/10.17632/n76t439f65.1.

Received 15.05.2022
Accepted 25.07.2022
Published 06.11.2022

Abdelkader Azzeddine Bengharbi[1], *PhD Student,*
Saadi Souad Laribi[1], *Doctor of Electrical Engineering,*
Tayeb Allaoui[1], *Professor of Electrical Engineering,*
Amina Mimouni[1], *PhD Student,*
[1] Energy Engineering and Computer Engineering (L2GEGI) Laboratory, University of Tiaret,
BP P 78 Zaâroura, 14000, Tiaret, Algeria.
e-mail: bengharbi.aek.azz@univ-tiaret.dz (Corresponding Author);
souad.laribi@univ-tiaret.dz;
tayeb.allaoui@univ-tiaret.dz;
amina.mimouni@univ-tiaret.dz

How to cite this article:
Bengharbi A.A., Laribi S., Allaoui T., Mimouni A. Photovoltaic system faults diagnosis using discrete wavelet transform based artificial neural networks. *Electrical Engineering & Electromechanics*, 2022, no. 6, pp. 42-47. doi: https://doi.org/10.20998/2074-272X.2022.6.07